Removal of interfering RLAN signals from C-band weather radar data

Krystian Specht[1,2], Katarzyna Ośródka[1], Jan Szturc[1], Włodzimierz Freda[2]

[1]Institute of Meteorology and Water Management – National Research Institute, Poland

[2]Gdynia Maritime University, Poland

krystian.specht@imgw.pl

RADVOL-QC System

The RADVOL-QC system performs quality control and corrections on raw 3-D data derived directly from the radars. The quality index (*QI*) ranges from 0 (poor quality) to 1 (excellent quality). This metric allows for an indirect but detailed assessment of the quality of the data. As the distance from the radar increases, the impact of interference grows, or some data is missing, the *QI* indicator decreases. The quality control mechanism offers a rapid and practical overview of the radar data's status, facilitating the timely identification of potential issues.

The Polish POLRAD radar network has been upgraded to 10 dual-polarisation C-band radars. Ensuring the corrected data is of exceptionally high quality is important, as it directly impacts the accuracy and reliability of meteorological models used in operational forecasting and analysis. High-quality data forms the backbone of these models, influencing predictions related to weather patterns, precipitation, and atmospheric dynamics. A comprehensive suite of 12 quality control and corrections algorithms has been meticulously designed and implemented to achieve this standard. These algorithms are tailored to identify and correct potential interferences in the data, such as attenuation, spikes, or any other noises, ensuring the information meets stringent operational requirements.

The algorithm for removing interfering RLAN signals (so-called spikes) in weather radar data is implemented in the Institute of Meteorology and Water Management – National Research Institute (IMGW) as a component of the RADVOL-QC system for the radar data quality control.

Detection of spikes

Detecting interferences caused by signals from the RLAN (5 GHz) network is done by evaluating the variability of echoes **along** and **across** the beam for each bin at various elevation angles. Detection methods ensure a comprehensive assessment of signal behaviour within the analysed area of 360 rays and 500 bins (using 0.5km resolution).

Subalgorithm (i) is designed to classify echoes based on their variance characteristics. An echo is identified as a spike if it is characterized by **low variance along** the beam and **high variance across** it. This classification criterion helps isolate interference patterns as follows:

$$\text{if } (var_{along} Z(\alpha,d) < 3) \text{ and } (var_{across} Z(\alpha,d) > 200) \rightarrow \text{there is a potential spike in } (\alpha,d) \tag{1}$$

where: var_{along} - variance calculated along the radar beam in $(\text{mm}^6\,\text{m}^{-3})^2$; var_{across} - variance calculated across the radar beam at a distance of up to ±6 or ±3 in dBZ^2; Z - radar reflectivity expressed in dBZ (across) or mm^6m^{-3} (along).

Subalgorithm (ii) is designed for detecting small-width spike echoes, i.e., not wider than 5°in azimuth. For each bin in which an echo was recorded ($Z(\alpha,d) > -32$ dBZ, which is the minimum reflectivity value detected by radars in the POLRAD network), $\Delta\alpha$ equal to 2° and 1° from azimuth α, while maintaining a constant distance d from radar [km]:

$$\begin{gathered}\text{if } ((Z(\alpha-\Delta\alpha,d) = -32\ dBZ) \text{ or } (Z(\alpha,d) - Z(\alpha-\Delta\alpha,d) > 20) \text{ or } (\text{potential spike in } Z(\alpha-\Delta\alpha,d))) \text{ and} \\ ((Z(\alpha+\Delta\alpha,d) = -32\ dBZ) \text{ or } (Z(\alpha,d) - Z(\alpha+\Delta\alpha,d) > 20) \text{ or } (\text{potential spike in } Z(\alpha+\Delta\alpha,d))) \\ \rightarrow \text{there is a potential spike in } (\alpha,d)\end{gathered} \tag{2}$$

After the analysis is completed, a verification process is carried out to confirm the identification of **real spike** echoes among those previously detected as **potential** ones. For each azimuth, the number of bins containing potential spike echoes of the following types is calculated: **wide (i)** and **narrow (ii)**. Based on this, if the number of bins in a given azimuth exceeds the defined thresholds, these echoes are recognized as real spikes, concluding the verification process. Each detected interference is assigned a **'spike' flag (*F*(α, *d*) = *spike*)**, which is used to identify disturbed echoes in correction algorithms. The Quality Index (*QI*) for bins within radar beams where any spike is detected is lowered only once at the moment the first disturbed echo is detected, following the order defined in the interference type pattern:

$$QI_{SPIKE}(\alpha,d) = \begin{cases} 0.2 & \text{detected wide } spike \text{ in bin} \\ 0.7 & \text{detected wide } spike \text{ in beam} \\ 0.5 & \text{detected narrow } spike \text{ in bin} \\ 0.8 & \text{detected narrow } spike \text{ in beam} \\ 1 & \text{no spike} \end{cases} \tag{3}$$

The map with quality index $QI_{SPIKE}(\alpha,d)$ serves as the basis for assessing the reliability of results in nowcasting models, for which radar data is a key component.

Correction of spikes

The presence of a spike in a bin with coordinates (α, *d*) is indicated by the 'spike' flag *F*(α, *d*) = *spike*. Based on this, **groups of neighbouring bins (α_{GROUP}, *d*)** are identified comprising bins located at the same distance *d*, within the azimuth range **$\alpha_i \le \alpha_{GROUP} \le \alpha_k$**, for which the flag $F(\alpha_{GROUP}, d)$ indicates the presence of a *spike* ($F(\alpha_{GROUP}, d)$ = *spike*). This range is determined iteratively by analysing consecutive bins to the left and right until the first bins without a detected spike are found in so-called **boundary bins** with coordinates (α_i–1, *d*) and (α_k+1, *d*).

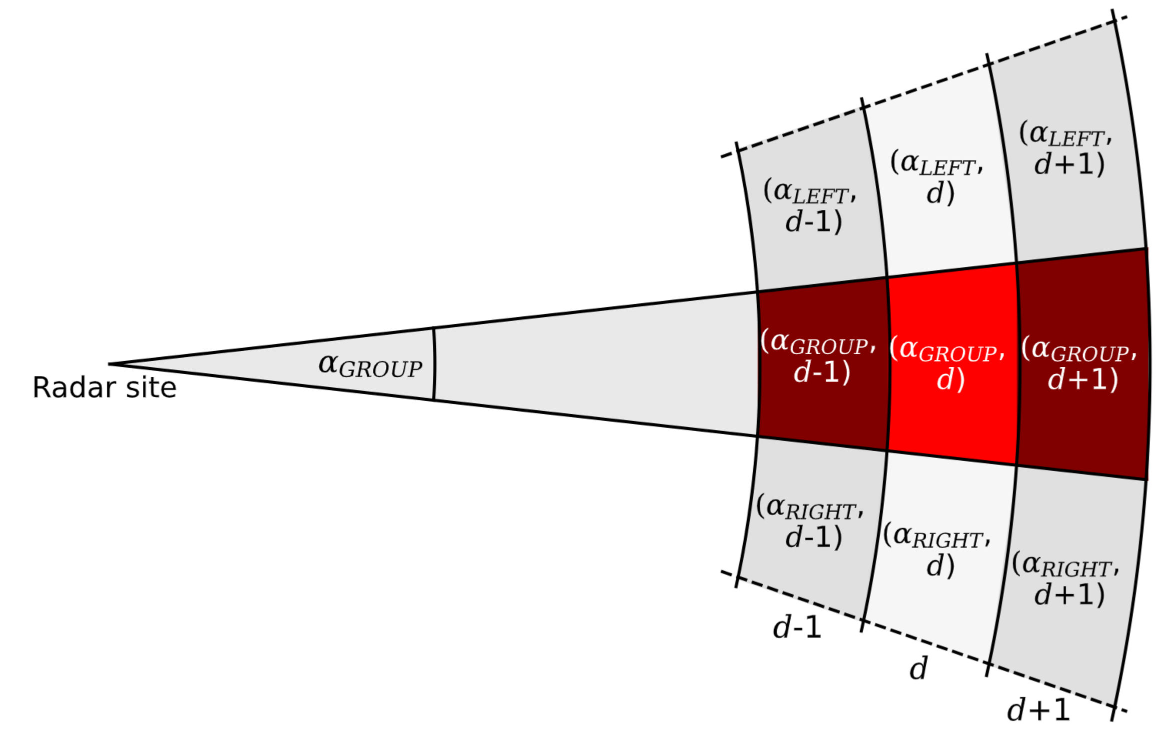

Fig. 1. A top-down view illustrating the analysis of the radar beam group's surroundings: the red area indicates the group with real spikes, while the maroon area represents the analysis of the neighbouring bin group at a distance of *d*±1. The grey and light grey areas denote the analysis of adjacent bin groups.

Reflectivity is analysed at three distances from the radar: at the distance where the group of spikes was detected (***d***) and in its close vicinity – i.e., at distances ***d*–1** and ***d*+1**. The analysis at neighbouring distances (*d*–1 or *d*+1) includes the same azimuth range (α_{GROUP}) defined by the group of spikes (α_{GROUP}, *d*). This means that the analysed area is extended across azimuths (α_{GROUP}) to the neighbouring distance (*d*–1 or *d*+1), provided that at least one echo not detected as *spike* is found in the bin range (α_{GROUP}, *d*–1) or (α_{GROUP}, *d*+1).

Reflectivity is also analysed in neighbouring azimuths, specifically within two groups next to the spike group (α_{GROUP}, *d*): **the left-hand group**, denoted as **(α_{LEFT}, *d*)**, which includes a sequence of bins with azimuths **$\alpha_i - m \le \alpha_{LEFT} \le \alpha_i - 1$**, and **the right-hand group**, denoted as **(α_{RIGHT}, *d*)**, which includes a sequence of bins with azimuths **$\alpha_k + 1 \le \alpha_{RIGHT} \le \alpha_k + m$**. The parameter ***m*** is a range of a group and can take on a value of 3 or 4 bins, depending on the reflectivity values observed in the boundary bins (see Figures 1 and 2, where grey and light-grey areas indicate the neighbourhood of real spikes).

a) Analysis area m =3

(α_i-3, d)	(α_i-2, d)	(α_i-1, d)	**(α_i, d)**	...	**(α_k, d)**	(α_k+1, d)	(α_k+2, d)	(α_k+3, d)

b) Analysis area m =3 with futher and nearer group of bins

(α_i-3, d+1)	(α_i-2, d+1)	(α_i-1, d+1)	**(α_i, d+1)**	...	**(α_k, d+1)**	(α_k+1, d+1)	(α_k+2, d+1)	(α_k+3, d+1)
(α_i-3, d)	(α_i-2, d)	(α_i-1, d)	**(α_i, d)**	...	**(α_k, d)**	(α_k+1, d)	(α_k+2, d)	(α_k+3, d)
(α_i-3, d-1)	(α_i-2, d-1)	(α_i-1, d-1)	**(α_i, d-1)**	...	**(α_k, d-1)**	(α_k+1, d-1)	(α_k+2, d-1)	(α_k+3, d-1)

c) Analysis area m =4

(α_i-4, d)	(α_i-3, d)	(α_i-2, d)	(α_i-1, d)	**(α_i, d)**	...	**(α_k, d)**	(α_k+1, d)	(α_k+2, d)	(α_k+3, d)	(α_k+4, d)

d) Analysis area m =4 with futher and nearer group of bins

(α_i-4, d+1)	(α_i-3, d+1)	(α_i-2, d+1)	(α_i-1, d+1)	**(α_i, d+1)**	...	**(α_k, d+1)**	(α_k+1, d+1)	(α_k+2, d+1)	(α_k+3, d+1)	(α_k+4, d+1)
(α_i-4, d)	(α_i-3, d)	(α_i-2, d)	(α_i-1, d)	**(α_i, d)**	...	**(α_k, d)**	(α_k+1, d)	(α_k+2, d)	(α_k+3, d)	(α_k+4, d)
(α_i-4, d-1)	(α_i-3, d-1)	(α_i-2, d-1)	(α_i-1, d-1)	**(α_i, d-1)**	...	**(α_k, d-1)**	(α_k+1, d-1)	(α_k+2, d-1)	(α_k+3, d-1)	(α_k+4, d-1)

Distance from radar (d)

Azimuth (α)

Fig. 2. a) Analysed area ±3 bins laterally from the analysed group of beams from (α_i, *d*) to (α_k, *d*); b) As above, additionally with analysis in a group of bins at a distance *d*±1 from the radar; c) Analysed area ±4 bins from the analysed group of beams from (α_i, *d*) to (α_k, *d*); d) As above, additionally with analysis in a group of bins at a distance *d*±1 from the radar.

Firstly, four bins on each side (*m*=4) of the group boundaries (α_i, α_k) are analysed to assess the percentage of *noecho* and *spike* bins (Equation 6).

$$L_{LEFT}(\alpha_i, d, m) = \sum_{\alpha=\alpha_i-m}^{\alpha_i-1} j(\alpha,d) \tag{4}$$

$$L_{RIGHT}(\alpha_k, d, m) = \sum_{\alpha=\alpha_k+1}^{\alpha_k+m} j(\alpha,d) \tag{5}$$

$$L(\alpha_i, \alpha_k, d, m) = \frac{L_{LEFT}(\alpha_i, d, m) + L_{RIGHT}(\alpha_k, d, m)}{2m} \cdot 100\% \tag{6}$$

$$\text{Where} \quad j(\alpha,d) = \begin{cases} 1, & (\alpha,d) \text{ SPIKE or } (\alpha,d) \text{ NOECHO} \\ 0, & (\alpha,d) \text{ not SPIKE and } (\alpha,d) \text{ not NOECHO} \end{cases}$$

If both boundary bins $Z(\alpha_i-1, d)$ and $Z(\alpha_k+1, d)$ contain meteorological echo and the surrounding area contains no more than 50% *spike*/*noecho* values, the group (α_{GROUP}, *d*) is replaced with the arithmetic mean:

$$Z(\alpha_{GROUP}, d) = \frac{Z(\alpha_i - 1,\ d) + Z(\alpha_k + 1,\ d)}{2} \tag{7}$$

If the threshold is exceeded, the group (α_{GROUP}, *d*) and surrounding bins are overwritten with *noecho* values (Equations 4 and 5), starting from the boundary bins.

If at least one of the boundary bins $Z(\alpha_i-1, d)$ or $Z(\alpha_k+1, d)$ equals *noecho*, the mean-based correction is skipped. Instead, the spike group (α_{GROUP}, *d*) is replaced with *noecho*. If the extended surroundings exceed a 25% threshold, surrounding bins in left and right groups (Equations 4 and 5) are also set to *noecho*.

Subsequently, the analysis is extended to the neighbouring distances *d*–1 and *d*+1. The value of the parameter *m* is 3 if both values in the boundary bins $Z(\alpha_i-1, d)$ and $Z(\alpha_k+1, d)$ are different from *noecho*. Otherwise, *m* is 4. If this percentage exceeds 50%, the surrounding bins are also replaced with *noecho*.

The final result is a cleaned radar reflectivity field, in which spike-type interferences have been more effectively reduced while preserving true precipitation echoes. In practice, this means delivering a radar image showing the actual area of precipitation without sudden and unjustified increases in reflectivity values.

Examples

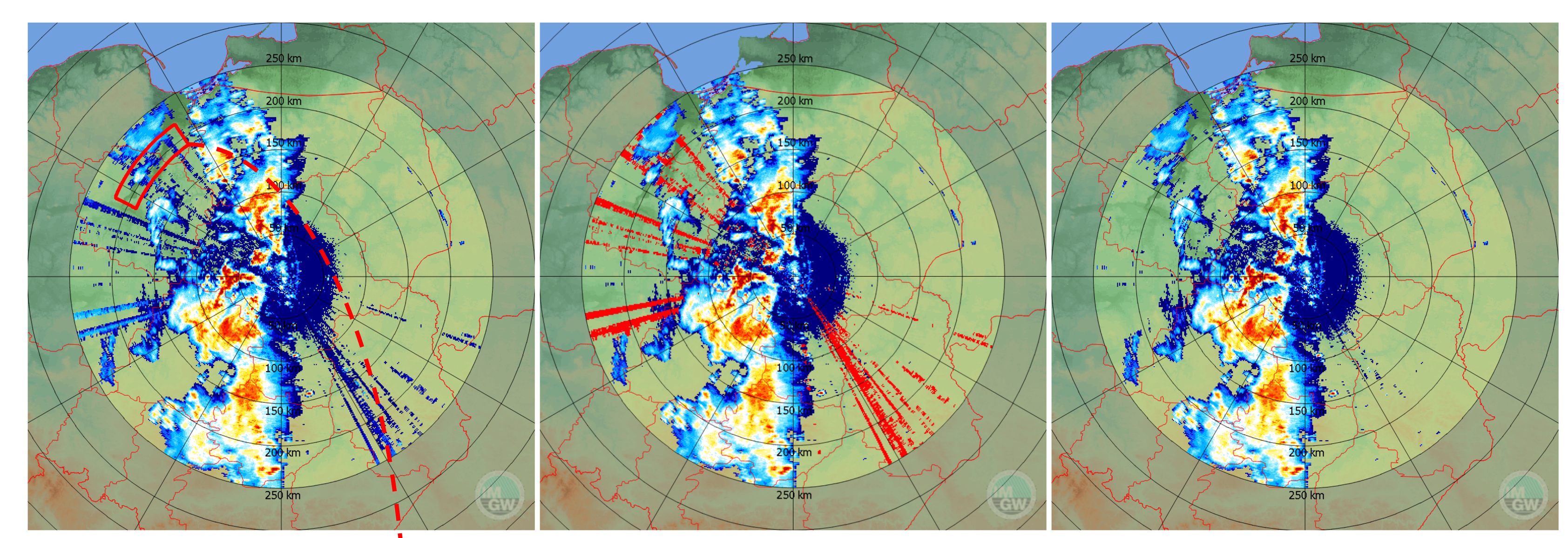

Fig. 3. CMAX product, analyse in cartesian coordinate system: a) Rawdata, red shows the analysed area; b) Detected spikes (red); c) Result of removing spikes.

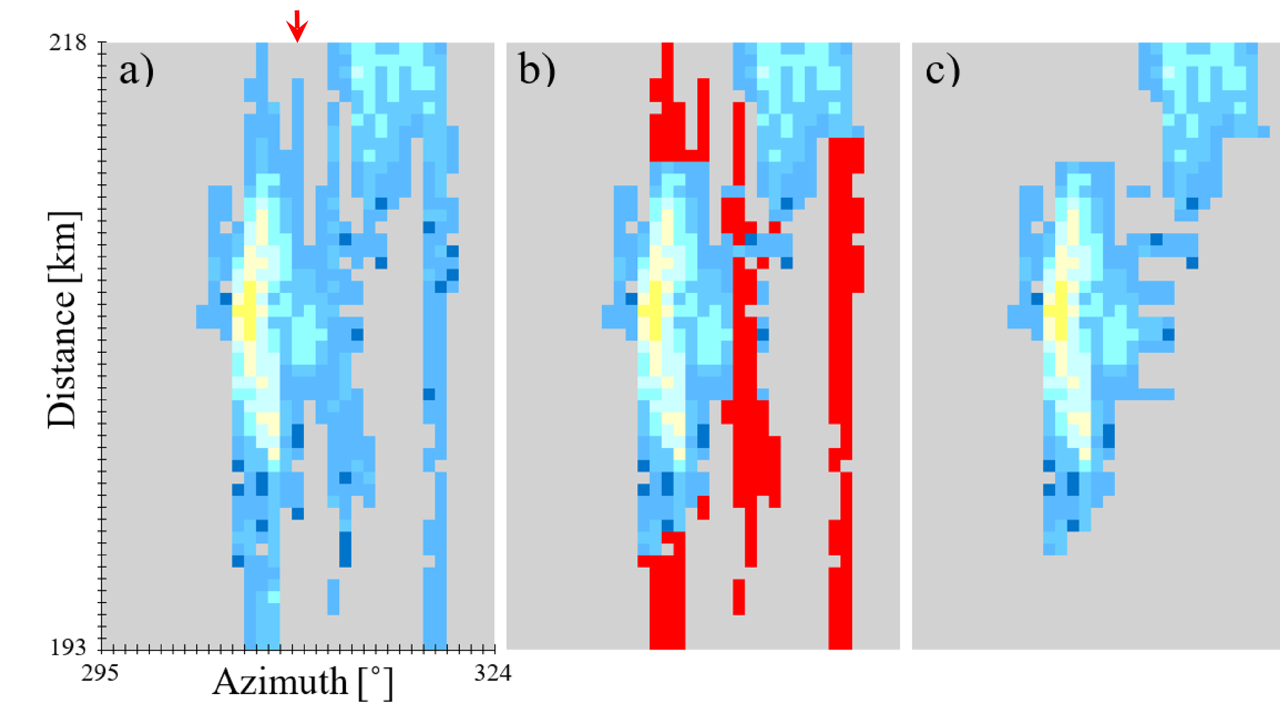

Fig. 4. Analysed area in polar coordinate system: a) Rawdata; b) Detected spikes (red); c) Result of removing spikes.